Aggregation Dependent Absorption Reduction of Indocyanine Green

R. Weigand,† F. Rotermund, and A. Penzkofer*

Institut II, Experimentelle und Angewandte Physik, Universität Regensburg, D-93040 Regensburg, Germany

Received: January 6, 1997; In Final Form: May 14, 1997[⊗]

Indocyanine green in water and in aqueous NaCl solutions forms large J-aggregate globules. With rising aggregate size the apparent absorption cross section per molecule decreases because of specific surface reduction of the aggregates. A theoretical description of the absorption behavior is given for dense spheres, loosely packed spheres (globules), straight chains, and coiled chains. The volume fill factor of the globules is determined from the absorption reduction measurements using the degree of aggregation from Mie scattering experiments described elsewhere.

1. Introduction

The organic dye indocyanine green[1] (ICG, also called cardiogreen[2] and IR125[3]) is widely applied in medical diagnosis[4,5] and it is a laser dye.[3] It forms large aggregates in water[6−8] and aqueous salts.[7] At room temperature a red-shifted J-aggregate absorption band[9,10] is formed within about two weeks in aqueous solution.[6,7] The J-aggregation is accelerated by heat treatment and salt (NaCl or NaI) addition.[11]

In this paper indocyanine green (ICG) J-aggregates in water and indocyanine green sodium iodide (ICG-NaI) J-aggregates in water and in aqueous NaCl solutions are prepared, and the absorption spectra are measured. With growing particle size an absorption decrease is observed. The dependence of the absorption strength on the degree of aggregation is addressed theoretically for dense spheres, loosely packed spheres, straight chains, and curled chains. The absorption reduction indicates the formation of three-dimensional particles (globules). The volume fill factor of the globules (loosely packed spheres) is deduced from the absorption reduction data using the degree of aggregation of the particles determined by Mie scattering experiments.[12]

The discussed phenomenon of attenuation reduction of absorbing chromophores (absorbing entities) with three-dimensional clustering is a quite general phenomenon and results from the reduction of the total cross-sectional area per unit volume with three-dimensional particle growth.[13,14] For strongly absorbing chromophores forming spheric clusters the attenuation reduction occurs already in the sub-nanometer and nanometer particle size range. In the case of transparent particles the light attenuation by Mie scattering decreases with particle growth for particle diameters large compared to the light wavelength (attenuation cross section becomes twice the particle cross section[15,16]) since again the specific surface (surface per unit volume) decreases with three-dimensional particle growth.[13,14]

2. Theory

The dependence of the absorption strength on the aggregation of chromophores (absorbing entities, Frenkel excitons in the case of J-aggregates[17,18]) is considered. Each chromophore may consist of n_{chr} molecules.

For single chromophore solutions the absorption coefficient, α_{chr}, is given by

$$\alpha_{chr}(\lambda) = \sigma_{chr}(\lambda)N_{chr} = f_{chr}(\lambda)A_{chr}N_{chr} = f_{chr}(\lambda)A_{chr}n_{chr}^{-1}N_m = \sigma'_{chr}(\lambda)N_m \quad (1)$$

where σ_{chr} is the absorption cross section of a single chromophore in solution and N_{chr} is the number density of chromophores. $N_{chr} = n_{chr}^{-1}N_m$, where N_m is the number density of molecules. A_{chr} is the cross-sectional area of a chromophore. $f_{chr} = \sigma_{chr}/A_{chr}$ is a proportionality factor, which we call chromophore absorption strength. λ is the wavelength in vacuum. $\sigma'_{chr} = \sigma_{chr}/n_{chr}$ is the normalized chromophore absorption cross section (apparent absorption cross-section of a molecule in a chromophore). The number density of molecules, N_m, has to be much less than $V_m^{-1} = (4\pi a_m^3/3)^{-1}$, where V_m is the molecule volume and a_m is the molecule radius, otherwise the bulk number density is approached and the solution and aggregation concept breaks down.

For a monodispersive aggregated chromophore solution with a degree of chromophore aggregation, β_{chr} (degree of molecule aggregation $\beta_m = \beta_{chr}n_{chr}$), the absorption coefficient, α_{ag}, is given by

$$\alpha_{ag}(\lambda) = \sigma_{ag}(\lambda)N_{ag} = f_{ag}(\lambda)A_{ag}N_{ag} \quad (2a)$$

$$= f_{ag}(\lambda)A_{ag}N_{chr}\beta_{chr}^{-1} = f_{ag}(\lambda)A_{ag}N_m\beta_m^{-1} \quad (2b)$$

$$= \sigma'_{ag}(\lambda)N_m \quad (2c)$$

In eq 2a $\sigma_{ag}(\lambda)$ is the absorption cross section of an aggregate and N_{ag} is the number density of the aggregates. A_{ag} is the cross-sectional area of an aggregate, and $f_{ag} = \sigma_{ag}(\lambda)/A_{ag}$ is a proportionality factor, which we call aggregate absorption strength. A_{ag} is shape dependent. In eq 2b the relations $N_{ag} = N_{chr}/\beta_{chr}$ and $N_{ag} = N_m/\beta_m$ are used. Equation 2c defines the normalized absorption cross section, σ'_{ag} (apparent absorption cross section of a molecule in an aggregate).

The aggregate absorption strength, $f_{ag} = \sigma_{ag}/A_{ag}$, is enhanced compared to the chromophore absorption strength, f_{chr}, by

$$f_{ag} = \frac{A_{ag}}{A_{chr}}f_{chr} = \frac{1 - \mathcal{T}_{ag}}{1 - \mathcal{T}_{chr}}f_{chr} \quad (3)$$

where $A_{ag} = 1 - \mathcal{T}_{ag}$ is the absorption degree of one aggregate, and $A_{chr} = 1 - \mathcal{T}_{chr}$ is the absorption degree of one chromophore. $\mathcal{T}_{chr}(\lambda) \approx \exp[-f_{chr}(\lambda)]$ is the transmission through one chromophore. $\mathcal{T}_{ag}$ is the transmission through one aggregate. It is shape dependent.

* Corresponding author.
† On leave from Departamento de Optica, Facultad de Ciencias Físicas, Universidad Complutense, 28040 Madrid, Spain.
⊗ Abstract published in *Advance ACS Abstracts,* September 1, 1997.

S1089-5639(97)00089-3 CCC: $14.00

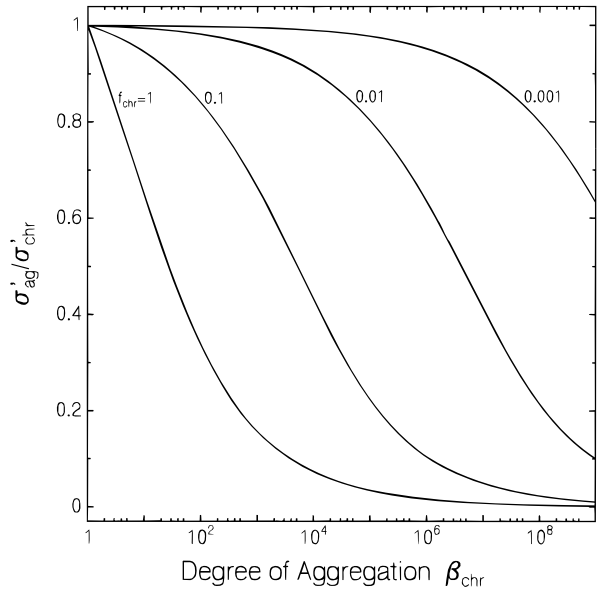

Figure 1. Illustration of aggregation dependent absorption behavior for dense cubes (eq 5). For the curves the chromophores absorption strength, f_{chr}, is varied.

The normalized aggregate absorption cross-section, $\sigma'_{ag}(\lambda)$, is obtained by insertion of eq 3 into eq 2b and by use of eq 1. One gets

$$\sigma'_{ag}(\lambda) = f_{ag}(\lambda)A_{ag}\beta_m^{-1} = \frac{1-\mathcal{T}_{ag}(\lambda)}{1-\mathcal{T}_{chr}(\lambda)} f_{chr}(\lambda)A_{ag}\beta_m^{-1} \tag{4a}$$

$$= \frac{1-\mathcal{T}_{ag}(\lambda)}{1-\mathcal{T}_{chr}(\lambda)} \frac{A_{ag}}{A_{chr}\beta_{chr}} \sigma'_{chr}(\lambda) \tag{4b}$$

For dense cubes (spheres) $A_{ag} \approx \beta_{chr}^{2/3}A_{chr}$ (area is proportional to the two-third power of volume) and $\mathcal{T}_{ag}(\lambda) \approx \exp[-f_{chr}(\lambda)\beta_{chr}^{1/3}]$ (light path through $\beta_{chr}^{1/3}$ chromophores). The absorption cross-section ratio, $\sigma'_{ag}(\lambda)/\sigma'_{chr}(\lambda)$, becomes

$$\frac{\sigma'_{ag}(\lambda)}{\sigma'_{chr}(\lambda)} \approx \frac{1-\exp[-f_{chr}(\lambda)\beta_{chr}^{1/3}]}{1-\exp[-f_{chr}(\lambda)]} \frac{1}{\beta_{chr}^{1/3}} \tag{5}$$

Equation 5 reveals that the normalized aggregate absorption cross section, σ'_{ag}, is practically the same as the normalized chromophore absorption cross section, σ'_{chr}, as long as $\beta_{chr}^{1/3}f_{chr}(\lambda) < 1$, i.e. as long as the total chromophoric absorption cross-sectional area per aggregate, $\beta_{chr}\sigma_{chr} = \beta_{chr}f_{chr}A_{chr}$, is less than the aggregate area, $A_{ag} \approx A_{chr}\beta_{chr}^{2/3}$. In this case the light penetrates the aggregates and each chromophore inside the aggregate is hit by the same amount of light. For $\beta_{chr}^{1/3}f_{chr}(\lambda) > 1$ the normalized aggregate absorption cross section decreases with rising β_{chr} toward $\sigma'_{ag} = \sigma'_{chr}/\{\beta_{chr}^{1/3}[1-\exp[-f_{chr}(\lambda)]]\}$. The reduction of σ'_{ag} with β_{chr} is caused by the reduction of the total geometric cross-sectional area with rising degree of aggregation.

In Figure 1 the absorption reduction due to aggregation in dense cubes is illustrated. The normalized absorption cross-section ratio, $\sigma'_{ag}/\sigma'_{chr}$, versus degree of aggregation, β_{chr}, is plotted for various chromophore absorption strengths, f_{chr}. In Figure 2 the change of spectral shape due to aggregation is illustrated. The dashed curve represents a homogeneously broadened Lorentzian line shape of 500 cm^{-1} spectral half-width (fwhm). A chromophore absorption strength of $f_{chr} = 0.1$ is assumed. The solid curves are calculated for various degrees of aggregation from $\beta_{chr} = 10$ to 10^7.

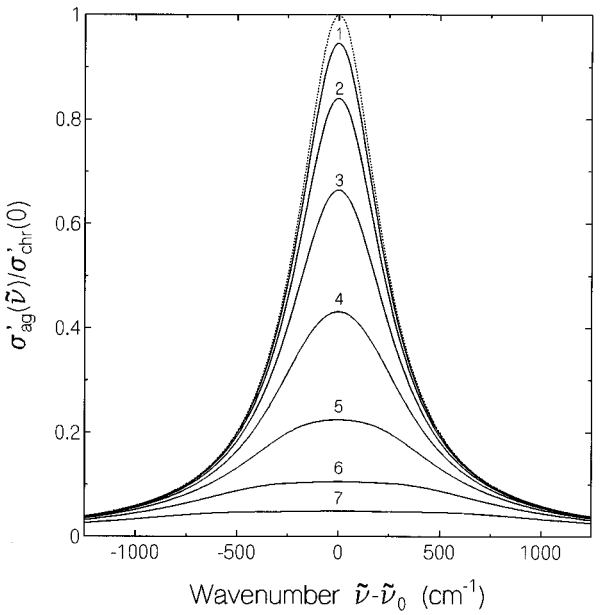

Figure 2. Theoretical reduction of normalized absorption cross section due to aggregation for dense spheric particles. Dotted curve: normalized chromophore absorption cross-section spectrum, $\sigma'_{chr}(\tilde{\nu})$, described by a Lorentzian shape of $\Delta\tilde{\nu}_{1/2} = 500$ cm^{-1} full spectral half-width. Solid curves: (1) $\beta_{chr} = 10$, (2) 100, (3) 1000, (4) 10^4, (5) 10^5, (6) 10^6, and (7) 10^7. A chromophore absorption strength of $f_{chr} = 0.1$ is assumed.

For loosely packed cubes (spheres) with a volume fill factor, κ_f, the aggregate cross-sectional area is $A_{ag} = \kappa_f^{-2/3}\beta_{chr}^{2/3}A_{chr}$ and $\mathcal{T}_{ag} \approx \exp[-f_{chr}(\lambda)\kappa_f^{2/3}\beta_{chr}^{1/3}]$ (number of chromophore layers is $\beta_{chr}/(\beta_{chr}/\kappa_f)^{2/3} = \kappa_f^{2/3}\beta_{chr}^{1/3}$)). The absorption cross-section ratio becomes

$$\frac{\sigma'_{ag}(\lambda)}{\sigma'_{chr}(\lambda)} \approx \frac{1-\exp[-f_{chr}(\lambda)\kappa_f^{2/3}\beta_{chr}^{1/3}]}{1-\exp[-f_{chr}(\lambda)]} \kappa_f^{-2/3}\beta_{chr}^{-1/3} \tag{6a}$$

$$\approx \frac{1-\exp[-f_{chr}(\lambda)\kappa_f^{2/3}\beta_{chr}^{1/3}]}{1-\exp[-f_{chr}(\lambda)\kappa_f^{2/3}]} \beta_{chr}^{-1/3} \tag{6b}$$

The approximation made in eq 6b gives $\sigma'_{ag}(\lambda)/\sigma'_{chr}(\lambda) = 1$ for $\beta_{chr} = 1$. As long as $f_{chr}\kappa_f^{2/3}\beta_{chr}^{1/3} < 1$, $\sigma'_{ag}(\lambda) \approx \sigma'_{chr}(\lambda)$. For $f_{chr}\kappa_f^{2/3}\beta_{chr}^{1/3} > 1$ the absorption cross-section ratio approaches $\sigma'_{ag}(\lambda)/\sigma'_{chr}(\lambda) = \{\kappa_f^{2/3}\beta_{chr}^{1/3}[1-\exp(-f_{chr}(\lambda))]\}^{-1}$. In Figure 3 $\sigma'_{ag}/\sigma'_{chr}$ is plotted versus β_{chr} for $f_{chr} = 1$ (dashed curves) and $f_{chr} = 0.1$ (solid curves) while the volume fill factors are set to $\kappa_f = 1$, 0.1, 0.01, and 0.001. The curves show that for the same absorption reduction the degree of aggregation has to be increased when the volume fill factor is reduced.

For rodlike (straight chain) aggregates with the rod axis at an angle of θ to the direction of the incident light, the aggregate area is given by $A_{ag}(\theta) = \max\{A_{chr}\beta_{chr}\sin(\theta), A_{chr}\}$ and the single aggregate transmission is given by $\mathcal{T}_{ag} = \max\{\exp[-f_{chr}(\lambda)/\sin(\theta)], \exp[-f_{chr}(\lambda)\beta_{chr}]\}$. The normalized absorption cross-section ratio becomes (eq 4b)

$$\frac{\sigma'_{ag}(\lambda,\theta)}{\sigma'_{chr}(\lambda)} = \frac{1-\max\{\exp[-f_{chr}(\lambda)/\sin(\theta)], \exp[-f_{chr}(\lambda)\beta_{chr}]\}}{1-\exp[-f_{chr}(\lambda)]} \max\{\sin(\theta), \beta_{chr}^{-1}\} \tag{7}$$

At $\theta = 0$,

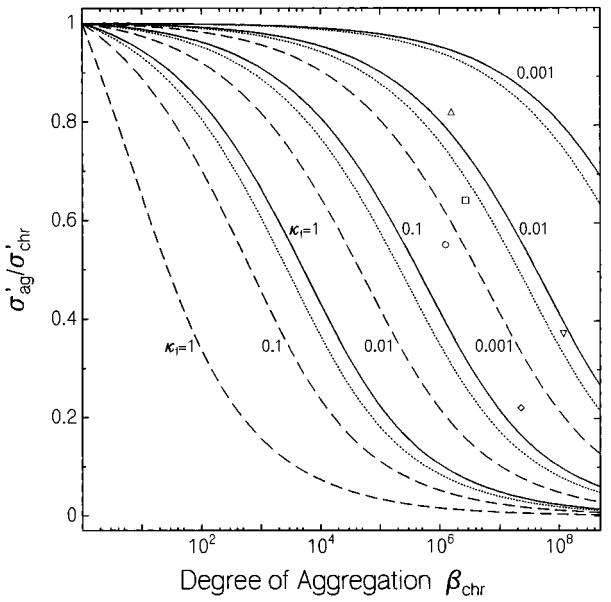

Figure 3. Influence of volume fill factor, κ_f, of loosely packed cubes (spheres) on absorption reduction. Normalized absorption cross-section ratio, $\sigma'_{ag}/\sigma'_{chr}$, versus degree of aggregation, β_{chr}, is presented. Dashed curves: chromophore absorption strength, $f_{chr} = 1$. Solid curves: $f_{chr} = 0.1$. Dotted curves: $f_{chr} = 0.126$. Symbols show experimental results for ICG in water (circle), ICG-NaI in water (triangle), ICG-NaI in 0.002 M (square), 0.01 M (diamond), and 0.05 M (inverted triangle) aqueous NaCl solution (β_{chr} data from ref 12).

$$\frac{\sigma'_{ag}(\lambda, 0)}{\sigma'_{chr}(\lambda)} = \frac{1 - \exp[-f_{chr}(\lambda)\beta_{chr}]}{1 - \exp[-f_{chr}(\lambda)]}\frac{1}{\beta_{chr}} \tag{8}$$

There is negligible absorption reduction for $f_{chr}(\lambda)\beta_{chr} < 1$, while the absorption reduction becomes very large for $f_{chr}(\lambda)\beta_{chr} > 1$, i.e. $\sigma'_{ag}(\lambda, 0) = \sigma'_{chr}(\lambda)/\{\beta_{chr}[1 - \exp[-f_{chr}(\lambda)]]\}$.

At $\theta = 90°$,

$$\frac{\sigma'_{ag}(\lambda, 90°)}{\sigma'_{chr}(\lambda)} = 1 \tag{9}$$

That is, there is no absorption reduction for rods aligned perpendicular to the light propagation direction.

An isotropic orientational rod distribution leads to (orientational averaging over θ)

$$\frac{\sigma'_{ag}(\lambda)}{\sigma'_{chr}(\lambda)} \approx \int_0^{\pi/2} \frac{1 - \exp[-f_{chr}(\lambda)/\sin(\theta)]}{1 - \exp[-f_{chr}(\lambda)]} \sin^2(\theta)\, d\theta \tag{10}$$

for $\beta_{chr} >> 1$. The ratio depends only weakly on $f_{chr}(\lambda)$. For $f_{chr} = 0.1$, $\sigma'_{ag}/\sigma'_{chr} = 0.98$, and for $f_{chr} = 1$, $\sigma'_{ag}/\sigma'_{chr} = 0.87$.

The absorption behavior of ideal coiled chains[19] (Gaussian chains,[19] random walk arrangement of segments) is discussed in the following using the model of loosely packed cubes. The Gaussian chain gyration volume is given by[19]

$$V_g = \frac{4\pi}{3}{a_g}^3 = \frac{4\pi}{3}\left(\frac{1}{6}\beta_{chr}{b_{chr}}^2\right)^{3/2} = \frac{4\pi}{3}\left(\frac{1}{6}\beta_{chr}{n_{chr}}^2{d_m}^2\right)^{3/2} \tag{11}$$

where $b_{chr} = n_{chr}d_m$ is the segment length of a chromophore and $d_m = 2a_m$ is the diameter of a molecule. The chromophore (absorbing entity) is taken to be a linear chain of n_{chr} molecules as is generally assumed for J-aggregates.[18] The tight packed

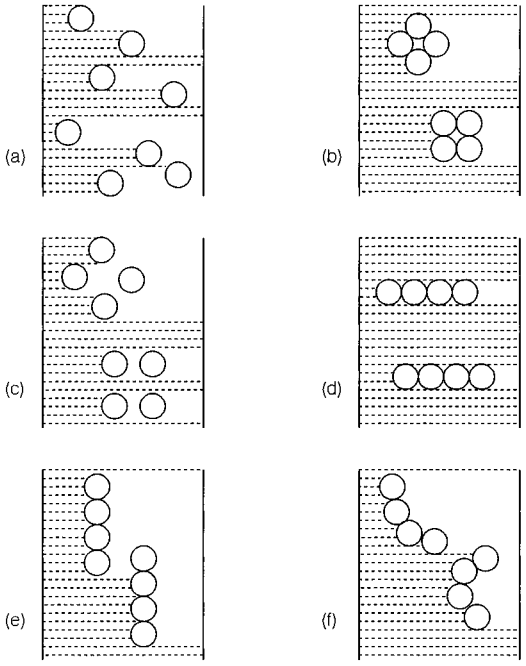

Figure 4. Illustration of transmission behavior of samples due to solute distribution: (a) isotropically distributed chromophores; (b) aggregation to dense cubes (spheres); (c) aggregation to loosely packed cubes (spheres); (d) aggregation to rodlike chromophore chains oriented parallel to light propagation direction, $\theta = 0°$; (e) aggregation to rodlike chromophore chains oriented perpendicular to light propagation direction, $\theta = 90°$; (f) aggregation to ideal chains (random walk chains).

volume is $V_t = \beta_{chr}n_{chr}4\pi{a_m}^3/3$. The volume fill factor, κ_f, is given by

$$\kappa_f = \frac{V_t}{V_g} = \left(\frac{3}{2}\right)^{3/2}\frac{1}{{n_{chr}}^2{\beta_{chr}}^{1/2}} \tag{12}$$

Insertion of eq 12 into eq 6 shows that the β_{chr} dependence cancels out, and one obtains $\sigma'_{ag}(\lambda)/\sigma'_{chr}(\lambda) \approx 1$.

For absorption reduction of coiled chains a densification (volume shrinkage compared to ideal chains) is necessary as it occurs in the coil−globule transition.[19]

The discussed absorption behavior of aggregates is illustrated in Figure 4. Spheric chromophores are displayed for simplicity, but the argumentation remains valid for more complex geometric chromophore shapes like rods. A large chromophore absorption degree, $A_{chr} \rightarrow 1$, is assumed (opaque chromophores) so that no light transmits through the chromophore areas. Part a of Figure 4 shows isotropically distributed chromophores. Light passes only through regions uncovered by the chromophores. In part b the chromophores have formed dense aggregated three-dimensional particles. The shrinkage of covered area and the increase of light passage are clearly seen. In part c loosely packed clusters are shown. The light passage is enhanced compared to part a, but it is reduced compared to part b. The picture d illustrates the situation of rodlike aggregates aligned parallel to the light propagation direction. A large absorption reduction compared to isotropically distributed single chromophores (part a) is clearly seen. In picture e the straight chains are aligned perpendicular to the light propagation direction. For this arrangement there occurs no absorption reduction. The picture f illustrates the absorption behavior of coiled chains. The absorption is nearly the same as in the case of isotropically distributed single chromophores.

For a polydispersive aggregated chromophore solution with distribution function $h(\beta_{chr})$ ($\int_0^\infty h(\beta_{chr})\, d\beta_{chr} = 1$) the normal-

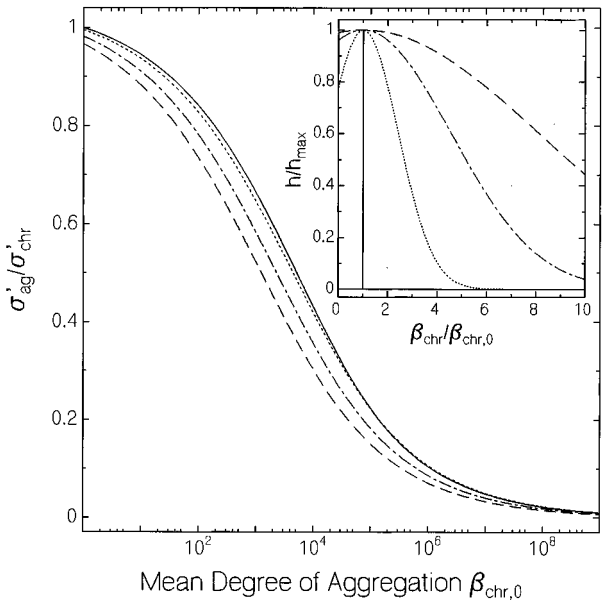

Figure 5. Influence of chromophore size distribution on absorption reduction. Truncated Gaussian distributions of the chromophore degree of aggregation are used as shown in the inset (eq 14). The line types of the main figure and the inset correspond to one another. Solid curve: $s_{chr} = 0$. Dotted curve: $s_{chr} = 2\beta_{chr,0}$. Dash-dotted curve; $s_{chr} = 5\beta_{chr,0}$. Dashed curve: $s_{chr} = 10\beta_{chr,0}$.

ized aggregate absorption cross section, $\sigma'_{ag}(\lambda)$ of eq 4b, changes to

$$\sigma'_{ag}(\lambda) = \sigma'_{chr}(\lambda)\int_0^\infty \frac{1 - \mathcal{T}_{ag}(\lambda)}{1 - \mathcal{T}_{chr}(\lambda)} \frac{A_{ag}}{A_{chr}\beta_{chr}} h(\beta_{chr})\, d\beta_{chr} \quad (13)$$

In Figure 5 the influence of polydispersivity on the absorption reduction is illustrated for dense cubes (eq 5). A truncated Gaussian distribution

$$h(\beta_{chr}) = \frac{\exp[-(\beta_{chr} - \beta_{chr,0})^2/s_{chr}^2]}{\int_0^\infty \exp[-(\beta_{chr} - \beta_{chr,0})^2/s_{chr}^2]\, d\beta_{chr}} \quad (14)$$

is used. Curves are shown for $f_{chr} = 0.1$ and $s_{chr} = 0$ (solid), $2\beta_{chr,0}$ (dotted), $5\beta_{chr,0}$ (dash-dotted), and $10\beta_{chr,0}$ (dashed). The distributions are shown by the inset in Figure 5. Up to $s_{chr} = 2\beta_{chr,0}$ there is practically no influence of the particle size spreading on the absorption reduction. For broader distributions ($s_{chr}/\beta_{chr,0} > 2$) some decrease of attenuation occurs compared to $s_{chr}/\beta_{chr,0} = 0$ (attenuation reduction effect of large particle dominates).

3. Experimental Section

The dyes indocyanine green from Acros, Pittsburgh (product name IR125, here called ICG), and indocyanine green sodium iodide (ICG-NaI) from Pulsion Medizintechnik, Munich, are investigated. The structural formulas of ICG and ICG-NaI are shown in Figure 6. ICG was dissolved in bidistilled water, while ICG-NaI was dissolved in bidistilled water and 2×10^{-3} M, 0.01 M, and 0.05 M aqueous NaCl solution. The investigated dye concentrations, C_{dye}, are listed in Table 1. For J-aggregate formation the dye solutions were heated to a temperature, ϑ_h, for a time period, t_h. The applied ϑ_h and t_h parameters are listed in Table 1. Without heating the formation of J-aggregates occurs very slowly. The dye concentration necessary for reasonable J-aggregate formation decreases with NaCl concentration. After formation the self-organized macromolecular aggregates are very stable, and the prepared highly concentrated solutions may be strongly diluted without dissolving the

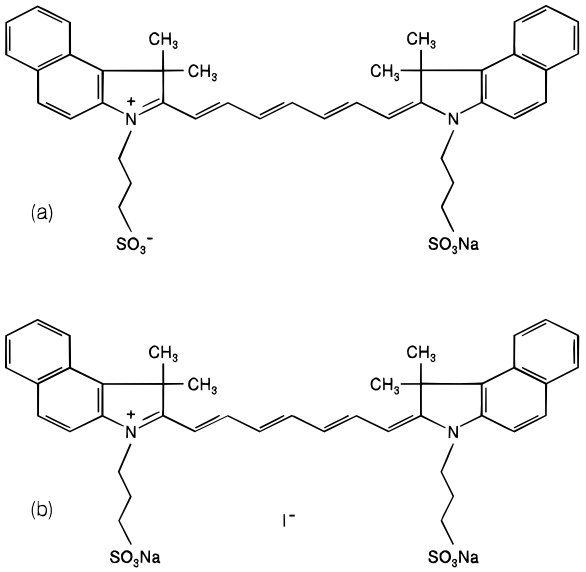

Figure 6. Structural formulas of (a) indocyanine green (ICG) and (b) indocyanine green sodium iodide (ICG-NaI).

J-aggregates within a time period of several hours at room temperature.[11]

The absorption cross-section spectra, $\sigma(\lambda)$, were determined from transmission measurements with a conventional spectrophotometer (Beckman ACTA M IV) by using the relation $\sigma = -\ln(T)/(N_m l)$, where T is the transmission, N_m is the molecule concentration, and l is the sample length. Dye cell thicknesses of $l = 2$ cm, 1 cm, 1 mm, 0.1 mm, 50 μm, and 10 μm were used depending on the dye concentration.

4. Results

In Figure 7 absorption cross-section spectra of ICG (dashed curves) and ICG-NaI (solid curves) in H_2O are shown. Spectra of freshly prepared samples of 1.5×10^{-5} and 1.5×10^{-3} M concentration are shown together with spectra of 1.5×10^{-3} M heat-treated solutions (see Table 1). At $C_{dye} = 1.5 \times 10^{-5}$ mol dm^{-3} the dye is dissolved predominantly in monomers (absorption peak at 775 nm) and dimers (peak at 710 nm).[8] With decreasing dye concentration the temporal dye stability decreases. At $C_{dye} = 1.5 \times 10^{-3}$ mol dm^{-3} the freshly prepared samples form higher oligomers which show up in modified absorption spectra with blue-shifted absorption peaks. The absorption cross-section spectra of the heat-treated samples have red-shifted J-bands of rather high peak absorption cross sections and rather small spectral half-widths. The wavelengths of maximum absorption, λ_{max}, the peak absorption cross sections, $\sigma(\lambda_{max})$, the S_0-S_1 absorption cross-section integrals, $\int_{S_0-S_1} \sigma(\bar{\nu})\, d\bar{\nu}$ (integration over wavenumber region of Figure 7), and the spectral half-widths, $\Delta\bar{\nu}_{1/2}$ (fwhm), are listed in Table 1. The absorption cross-section spectra of the strongly diluted solutions of ICG-NaI (curve 1″) and ICG (curve 2″) are practically the same, while the peak absorption cross section, σ(890 nm), of the ICG J-aggregates (curve 2) is lower than that of the ICG-NaI J-aggregates (curve 1).

In Figure 8 absorption cross-section spectra of ICG-NaI in aqueous NaCl solutions are shown. The NaCl concentration was varied from $C_{NaCl} = 0.002$ mol/dm^3 to $C_{NaCl} = 0.05$ mol/dm^3 (see Figure caption 8 and Table 1). The dye concentration of the heat-treated (curves 1, 2, 3) and the corresponding freshly prepared samples (curves 1′, 2′, 3′) was changed with NaCl concentration. The curve 1″ belongs to a freshly prepared sample of $C_{dye} = 2 \times 10^{-6}$ mol/dm^3 and $C_{NaCl} = 0.002$ mol/dm^3. At low NaCl concentration and low dye concentration (curve 1″) the spectrum is dominated by monomer absorption.

TABLE 1: Preparation Data and Spectroscopic Results

	ICG			ICG-NaI							
C_{NaCl} (mol dm^{-3})	0	0	0	0	0	0	0.002	0.002	0.01	0.01	0.05	0.05
C_{dye} (mol dm^{-3})	1.5×10^{-3}	1.5×10^{-3}	1.5×10^{-5}	1.5×10^{-3}	1.5×10^{-3}	1.5×10^{-5}	5.6×10^{-4}	2×10^{-6}	5×10^{-4}	5×10^{-4}	10^{-4}	10^{-4}
ϑ_h (°C)	65	20	20	65	20	20	65	20	55	20	45	20
t_h (h)	32	0	0	32	0	0	43	0	65	0	120	0
λ_{max} (nm)	886	677	772	890	696	780	893	697	891	693	893	697
$\sigma(\lambda_{max})$ (cm^2)	7.6×10^{-16}	3.8×10^{-16}	7.8×10^{-16}	1.14×10^{-15}	4.5×10^{-16}	7.9×10^{-16}	8.9×10^{-16}	4.95×10^{-16}	8.1×10^{-16}	5.1×10^{-16}	4.7×10^{-16}	3×10^{-16}
$\int_{S_0-S_1}\sigma(\tilde{\nu})\,d\tilde{\nu}$ (cm)	1.14×10^{-12}	1.2×10^{-12}	1.7×10^{-12}	1.4×10^{-12}	9.9×10^{-13}	1.7×10^{-12}	9.5×10^{-13}	1.04×10^{-12}	1.45×10^{-12}	6.4×10^{-13}	9.7×10^{-13}	9.8×10^{-13}
$\Delta(\tilde{\nu})_{1/2}$ (cm^{-1})	640	3240	2030	520	1660	2070	480	1540	1090	540	1600	1080	3100
$\sigma(\lambda_{max})/\sigma'_{chr}(\lambda_{max})$	0.55			0.82			0.64			0.37		0.22	
$\bar{\beta}_m$ [a]	$\sim 2 \times 10^7$			$\sim 2.5 \times 10^7$			$\sim 4.3 \times 10^7$			$\sim 1.9 \times 10^9$		$\sim 3.7 \times 10^8$	
$\bar{\beta}_{chr}$ [b]	$\sim 1.3 \times 10^6$			$\sim 1.6 \times 10^6$			$\sim 2.7 \times 10^6$			$\sim 1.2 \times 10^8$		$\sim 2.3 \times 10^7$	
κ_f	0.033			0.005			0.013			0.008		0.045	
$\bar{a}_g$ (nm)	~500			~720			~670			~3200		~1400	

[a] From ref 12. [b] $\bar{\beta}_{chr} = \bar{\beta}_m/n_{chr}$, $n_{chr} = 16$, from ref 26.

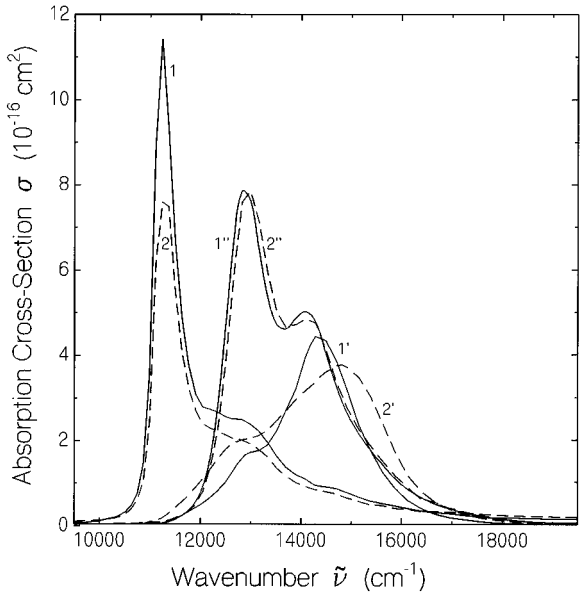

Figure 7. Absorption cross-section spectra of ICG (dashed curves) and ICG-NaI (solid curves) in H_2O. Curves 1, 2: J-aggregates prepared by heat treatment, concentration of preparation 1.5×10^{-3} mol/dm^3, concentration of measurement 1.5×10^{-5} mol/dm^3. Curves 1′, 2′: freshly prepared samples, $C_{dye} = 1.5 \times 10^{-3}$ mol/dm^3. Curves 1″, 2″: freshly prepared samples, $C_{dye} = 1.5 \times 10^{-5}$ mol/dm^3.

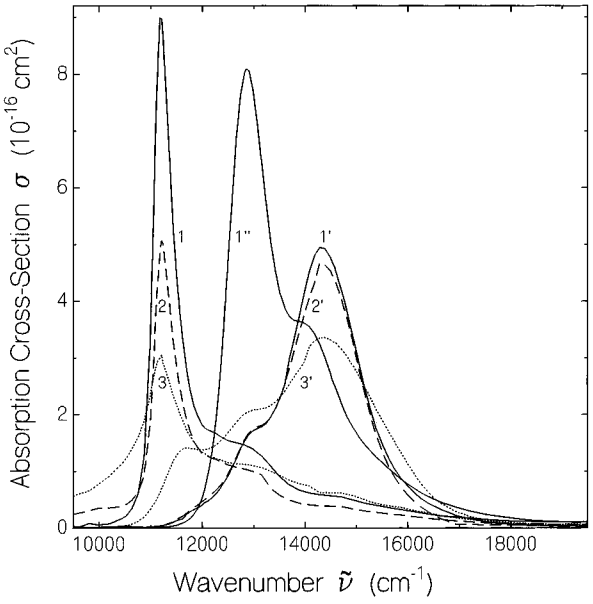

Figure 8. Absorption cross-section spectra of ICG-NaI in 0.002 M (solid curves), 0.01 M (dashed curves), and 0.05 M (dotted curves) aqueous sodium chloride solution. Curves 1, 2, 3: J-aggregates prepared by heat treatment, $C_{dye} = 5.6 \times 10^{-4}$ mol/dm^3 (1), 5×10^{-4} mol/dm^3 (2), 1×10^{-4} mol/dm^3 (3). Curves 1′, 2′, 3′: freshly prepared samples, $C_{dye} = 5.6 \times 10^{-4}$ mol/dm^3 (1′), 5×10^{-4} mol/dm^3 (2′), and 1×10^{-4} mol/dm^3 (3′). Curve 1″: freshly prepared sample, $C_{dye} = 2 \times 10^{-6}$ mol/dm^3.

With rising NaCl concentration and rising dye concentration, dimerization and higher oligomer formation dominate in the freshly prepared samples. The absorption cross-section peak of the J-aggregates (curves 1, 2, 3) decreases with rising NaCl concentration, indicating an increasing particle size with rising sodium chloride concentration (see below).[12] The short-wavelength absorption cross-section tails are expected to belong to the J-aggregates.[11,20] The relevant absorption cross-section parameters are collected in Table 1.

5. Data Analysis

The absorption reduction at the wavelength, $\lambda_{max} = 890$ nm, of peak J-band absorption is considered.

For the determination of the absorption cross-section ratio, $\sigma'_{ag}(\lambda_{max})/\sigma'_{chr}(\lambda_{max})$, the normalized chromophore absorption cross section, $\sigma'_{chr}(\lambda_{max})$, is needed. It is determined approximately by assuming that the true absorption cross-section integral is the same for the dilute freshly prepared dye solution and the heat-treated J-aggregates.[21−24] The relation $\sigma'_{chr}(\lambda_{max}) = \sigma(\lambda_{max}) \int_{S_0-S_1} \sigma_f(\bar{\nu})\, d\bar{\nu} / \int_{S_0-S_1} \sigma_h(\bar{\nu})\, d\bar{\nu}$ is used, where $\sigma_h(\bar{\nu})$ is the absorption cross-section spectrum of the 1.5×10^{-3} M heat-treated ICG-NaI solution in water (solid curve 1 in Figure 7) and $\sigma_f(\bar{\nu})$ is the absorption cross-section spectrum of the freshly prepared 1.5×10^{-5} M ICG-NaI solution in water (solid curve 1″ in Figure 7). A value of $\sigma'_{chr}(\lambda_{max}) = 1.39 \times 10^{-15}$ cm^2 is obtained. The $\sigma'_{ag}(\lambda_{max})/\sigma'_{chr}(\lambda_{max})$ values are listed in Table 1.

The chromophore absorption strength, $f_{chr}(\lambda_{max}) = \sigma'_{chr}(\lambda_{max}) \cdot n_{chr}/A_{chr}$ (eq 1), is approximately equal to $f_{chr}(\lambda_{max}) = \sigma'_{chr}(\lambda_{max})/A_m$ assuming linear chains of n_{chr} molecules forming the chromophores[18,25] (see eqs 7−10: $A_{chr} = n_{chr}A_m$). The geometric cross-sectional area, A_m, of an ICG-NaI molecule has been determined from density measurements of the dye stuff ($\rho_{dye} = 1.3$ g/cm^3) using the relations $V_m = 0.74 M_{dye}/(\rho_{dye} N_A)$, $a_m = [3V_m/(4\pi)]^{1/3}$, and $A_m = \pi a_m^2$, where 0.74 is the fill factor of hexagonal close-packed spheres, $M_{dye} = 924.87$ g/mol is the molar mass of ICG-NaI, and N_A is the Avogadro constant. A value of $A_m = 1.1 \times 10^{-14}$ cm^2 ($d_m = 2a_m = 1.19$ nm) is obtained. The same values of A_m and d_m are assumed for ICG. For our indocyanine green J-aggregates we obtain $f_{chr}(\lambda_{max}) = \sigma'_{chr}(\lambda_{max})/A_m = 0.126$.

The absorption cross-section ratio, $\sigma'_{ag}(\lambda_{max})/\sigma'_{chr}(\lambda_{max})$, of globules depends on $f_{chr}(\lambda_{max})$, β_{chr}, and κ_f (eq 6). $\beta_{chr} = \beta_m/n_{chr}$. The average monomer degree of aggregation, $\bar{\beta}_m$, of the investigated J-aggregates has been determined previously by light scattering experiments.[12] The number of molecules, n_{chr}, forming a chromophore has been determined by femtosecond laser saturable absorption studies.[26] A value of $n_{chr} \approx 16$ was found. The obtained $\bar{\beta}_m$ and $\bar{\beta}_{chr}$ values are listed in Table 1. The determination of κ_f is addressed here. In Figure 3 the dotted curves display $\sigma'_{ag}(\lambda_{max})/\sigma'_{chr}(\lambda_{max})$ curves versus β_{chr} for the experimental situation of $f_{chr}(\lambda_{max}) = 0.126$. The κ_f values of the curves are 1, 0.1, 0.01, and 0.001. The experimental $\sigma'_{ag}(\lambda_{max})/\sigma'_{chr}(\lambda_{max})$ and $\bar{\beta}_{chr}$ data pairs are marked in Figure 3. The best fitting κ_f values are listed in Table 1. The average globule radii, $\bar{a}_g = [3V_g/(4\pi)]^{1/3} = [3\bar{\beta}_m V_m/(4\pi\kappa_f)]^{1/3}$, are included in Table 1.

6. Discussion

Compared to the high degree of chromophore aggregation, the absorption reduction is moderate. Therefore small volume fill factors and large radii of the globules are obtained. ICG in water and ICG-NaI in water have about the same degree of aggregation, but ICG in water is more tightly packed. With rising NaCl concentration the packing density increases.

The spectral half-width, $\Delta\bar{\nu}_{1/2}$, of the red-shifted absorption band increases with rising degree of aggregation and volume fill factor, as is expected from the absorption strength dependent absorption reduction of aggregates (see Figure 2). In the wings the absorption strength, $f_{chr}(\lambda)$, is smaller and therefore the aggregate size dependent absorption reduction is smaller.

The absorption cross-section spectra in the spectral wings of curves 2 and 3 in Figure 8 differ from the expectations of Figure 2. The enhanced apparent absorption in the long-wavelength region is due to scattering losses, as has been verified by Mie scattering investigations.[12]

Spongy particles up to about 10 μm in size have been observed for all samples in an optical microscope. The number density of the micrometer size particles increased strongly with NaCl concentration.

7. Conclusions

The reduction of absorption with increasing particle size and volume fill factor of indocyanine green J-aggregates has been studied. The absorption reduction is caused by specific surface reduction with growing particle size.[13,14] The effect is readily observed for molecules in wavelength regions of high absorption strength (high chromophore absorption cross section). Theoretical relations between the degree of aggregation and the absorption behavior were developed for dense and loosely packed spheric particles as well as for rodlike chains and flexible coiled chains. The observed absorption reduction indicates a globule formation which may be approximated by loosely packed spherical particle formation. Using degree of aggregation data from Mie scattering experiments,[12] volume fill factors of the globules could be determined from the absorption reduction studies.

The described phenomenon of apparent absorption cross-section reduction due to aggregation should be generally considered in absorption spectroscopic studies of aggregate and polymer solutions consisting of chromophoric units of high absorption strength.

Acknowledgment. R.W. gratefully acknowledges the FPU grant received from the Ministerio de Educacion y Ciencia (Spain) for this research.

References and Notes

(1) Fox, I. J.; Brooker, I. G. S.; Heseltine, D. W.; Essex, H. E.; Wood, E. H. *Am. J. Physiol.* **1956**, *187*, 599.
(2) Michie, D. D.; Goldsmith, R. S.; Mason, A. D., Jr. *Proc. Soc. Exptl. Biol. Med.* **1962**, *111*, 540.
(3) Pierce, B.; Birge, R. *IEEE J. Quantum Electron.* **1982**, *18*, 1194.
(4) Fox, I. J.; Wood, E. H. *Mayo Clin. Proc.* **1960**, *35*, 732.
(5) Nahimisa, T. *Tokai J. Exp. Clin. Med.* **1982**, *7*, 419.
(6) Baker, K. J. *Proc. Soc. Exp. Biol. Med.* **1966**, *122*, 957.
(7) Landsman, M. L. J.; Kwant, G.; Mork, G. A.; Zylstra, W. G. *J. Appl. Physiol.* **1976**, *40*, 575.
(8) Philip, R.; Penzkofer, A.; Bäumler, W.; Szeimies, R. M.; Abels, C. *J. Photochem. Photobiol. A: Chem.* **1996**, *96*, 137.
(9) Scheibe, G. *Angew. Chem.* **1937**, *50*, 51.
(10) Jelley, E. E. *Nature* **1936**, *138*, 1009.
(11) Rotermund, F.; Weigand, R.; Penzkofer, A. *Chem. Phys.*, to be published.
(12) Weigand, R.; Rotermund, F.; Penzkofer, A. *Chem. Phys.*, to be published.
(13) Gregg, S. D.; Sing, K. S. W. *Adsorption, Surface Area and Porosity*; Academic Press: London, 1967.
(14) Lowell, S.; Shields, J. E. *Powder Surface Area and Porosity*, 3rd ed.; Chapman & Hall: London, 1991.
(15) Struve, O *Ann. Astrophys.* **1938**, *1*, 143.
(16) van de Hulst, H. C. *Light Scattering by Small Particles*; John Wiley & Sons: New York, 1957.
(17) Möbius, D. *Adv. Mater.* **1995**, *7*, 437.
(18) Spano, F. C.; Mukamel, S. *J. Chem. Phys.* **1989**, *91*, 683.
(19) Doi, M. *Introduction to Polymer Physics*; Clarendon Press: Oxford, 1996.
(20) Dorn, H. P.; Müller, A. *Chem. Phys. Lett.* **1986**, *130*, 426.
(21) Fidder, H.; Terpstra, J.; Wiersma, D. A. *J. Chem. Phys.* **1991**, *94*, 6895.
(22) Knoester, J. *J. Chem. Phys.* **1993**, *99*, 4866.
(23) Spano, F. C. *Nonlinear Opt.* **1995**, *12*, 275.
(24) Knapp, E. W. *Chem. Phys.* **1984**, *85*, 73.
(25) Stiel, H.; Voigt, B.; Hirsch, J.; Teuchner, K.; Leupold, D. *Adv. Mater.* **1995**, *7*, 445.
(26) Wittmann, M.; Rotermund, F.; Weigand, R.; Penzkofer, A. *Appl. Phys. B*, to be published.
(27) Bohren, C. F.; Huffman, D. R. *Absorption and Scattering of Light by Small Particles*; Wiley: New York, 1983.